Title: Membrane compartmentalization of mycobacterial peptidoglycan synthesis

Authors: Alam García-Heredia[1], Julia Puffal[2], Julius Judd[3] *, Todd A. Gray[3,4], Yasu S. Morita[1,2, †], M. Sloan Siegrist[1,2, †]

Affiliations:

[1]Molecular and Cellular Biology Graduate Program, University of Massachusetts, Amherst, MA 01003, USA.

[2]Department of Microbiology, University of Massachusetts, Amherst, MA 01003, USA.

[3]Division of Genetics, Wadsworth Center, New York State Department of Health, Albany, NY 12208, USA.

[4]Department of Biomedical Sciences, University at Albany, Albany, NY 12208, USA.

* Current address: Department of Molecular Biology and Genetics, Cornell University, Ithaca, NY 14853, USA.

† Corresponding author. Email: siegrist@umass.edu (M.S.S.); ymorita@microbio.umass.edu (Y.S.M.).

Abstract: Cell wall peptidoglycan, a mesh of polysaccharides crosslinked by short peptides, encases the bacterial cell and protects it from turgor pressure lysis.

Peptidoglycan synthesis is an effective antibiotic target. Assembly of the biopolymer occurs in close association with the plasma membrane, but higher order organization of the process has not been described. In mycobacteria, intracellular membrane domains comprise biochemically and spatially distinct regions within the conventional plasma membrane. We find that lipid-linked peptidoglycan precursors are made in these domains and then trafficked to the conventional plasma membrane for insertion into the cell wall. Disorganization of the membrane rapidly delocalizes and then halts peptidoglycan assembly. Our data show that membrane compartmentalization is an essential feature of mycobacterial cell wall biogenesis.

Main Text: Many antibiotics target peptidoglycan synthesis, a well-conserved pathway that spans the cytoplasm, plasma membrane and periplasm. The polyprenol-linked, disaccharide-pentapeptide monomer lipid II is completed by the glycosyltransferase MurG in the inner leaflet of the plasma membrane (Fig. 1A). Lipid II is then flipped to the outer leaflet by MurJ and integrated into the cell wall by membrane-bound transglycosylases and transpeptidases from the penicillin-binding protein (PBP) and shape, elongation, division, and sporulation (SEDS) families (*1-4*).

The plasma membrane is a heterogeneous mixture of lipids and proteins. Mycobacteria, for example, have **i**ntracellular **m**embrane **d**omains (IMD, formerly called the PMf (*5*) for **p**lasma **m**embrane **f**ree of cell wall) that are separable from the conventional plasma membrane (designated the PM-CW, for **p**lasma **m**embrane tightly associated with **c**ell **w**all) by sucrose density gradient fractionation. The proteome and lipidome of IMD are distinct from PM-CW (*5, 6*). While PM-CW-resident proteins localize

47 along the perimeter of live mycobacteria, IMD-resident proteins localize along sidewall
48 but are enriched adjacent to sites of polar cell elongation (*6, 7*).
49 Our proteomics analysis indicated that MurG is present in the IMD while
50 sequentially-acting PBPs preferentially associate with the PM-CW (*6*). We also
51 observed *in situ* that the subpolar enrichment of MurG-RFP resembles that of the
52 validated IMD marker mCherry-GlfT2 or GlfT2-GFP (*6, 8*) but that nascent cell wall at
53 the mycobacterial poles primarily abuts rather than colocalizes with mCherry-GlfT2 (*7*).
54 These observations suggest that lipid II synthesis is biochemically and spatially
55 segregated from the subsequent steps of cell wall assembly (Fig. 1A).
56 We expressed a functional MurG-Dendra2 fusion in *Mycobacterium smegmatis*
57 (Fig. S1) and assayed its distribution in membrane fractions that had been separated by
58 density gradient (Fig. 1B). The fusion to MurG, a peripheral membrane protein, was
59 enriched in both the cytoplasmic and IMD membrane fractions (Fig. 1C; Fig. S2),
60 recapitulating the association predicted for the native protein (*6*). In intact cells, polar
61 enrichment of MurG-Dendra2 was coincident with that of mCherry-GlfT2 (Fig. 1D). The
62 spatial relationship between the proteins was similar to that of MurG-RFP and GlfT2-
63 GFP (*8*), suggesting that it is independent of the fluorescent protein tag.
64 The association of MurG with the IMD, but not with the PM-CW, implied that the
65 membrane domain is the site of lipid II synthesis. We refined an *in vitro* D-amino acid
66 exchange assay to detect lipid-linked peptidoglycan precursors from *M. smegmatis*
67 membrane fractions (*9, 10*). In wildtype cells, we detected biotinylated molecules in both
68 the IMD and PM-CW (Fig. 2B; Fig. S2). We hypothesized that the labeled species
69 comprised precursors in the inner leaflet of the plasma membrane as well as lipid II that

70 had been flipped to the outer leaflet. We, and others, have shown that depletion of MurJ
71 results in an accumulation of biotinylated precursors (*10, 11*). By performing the D-
72 amino acid exchange reaction on membrane fractions, we found that precursors
73 accumulate in the IMD (Fig. 2B; Fig. S2). These results suggest that lipid II is made in
74 the IMD and transferred to the PM-CW in a MurJ-dependent manner.

75 PBPs and SEDS proteins incorporate lipid II into peptidoglycan. Given the
76 trafficking of precursors from the IMD to the PM-CW (Fig. 2B) and the association of cell
77 wall fragments specifically with the PM-CW (*5*), we hypothesized that extracellular,
78 peptidoglycan-acting enzymes function in the PM-CW. While our proteomics did not
79 detect SEDS proteins, our PM-CW dataset was enriched for all of the known
80 mycobacterial PBPs (*6*). Fluorescent derivatives of β-lactam antibiotics such as Bocillin-
81 FL bind covalently to PBPs and can be used to image transpeptidase-active enzymes in
82 both polyacrylamide gels and intact cells. We incubated membrane fractions from
83 wildtype *M. smegmatis* with Bocillin-FL and identified fluorescent proteins in the PM-CW
84 but not the IMD (Fig. 2B; Fig. S2). As expected for PBPs, the signal from these bands
85 was diminished by pre-treatment with the β-lactam ampicillin (Fig. S4). We focused on
86 characterizing PonA1, a bifunctional transglycosylase/transpeptidase that is essential
87 for *M. smegmatis* growth (*12, 13*). Depletion of PonA1 (*12*) resulted in the loss of the
88 highest molecular fluorescent band (Fig. S4), confirming that this protein is present and
89 active specifically in the PM-CW (Fig. 2B). We next expressed a functional PonA1-
90 mRFP fusion in *Mycobacterium smegmatis* (*13*) and found that it was more evenly
91 distributed around the cell perimeter than MurG-Dendra2, and in a manner similar to the
92 functional PM-CW marker PimE-GFP (Fig. 2C, Fig. S5; (*6*). Together, our data show

93 that MurG and PonA1 occupy spatially distinct compartments along the pathway of
94 peptidoglycan synthesis.

95 Based on our biochemical data, we hypothesized that lipid II incorporation into
96 the cell wall is laterally segregated from its synthesis. We previously showed that
97 alkynyl and azido D-amino acid dipeptides (*14*) incorporate into lipid-linked
98 peptidoglycan precursors in *M. smegmatis* (*10*) and that metabolic labeling with alkynyl
99 dipeptide (alkDADA or EDA-DA) is most intense in regions adjacent to the IMD marker
100 mCherry-GlfT2 (*7*). We labeled MurG-Dendra2-expressing *M. smegmatis* with alkDADA
101 for ~1% of generation time and detected the presence of the alkyne by copper-
102 catalyzed azide-alkyne cycloaddition (CuAAC; Fig 2D; (*10*). To tune our detection for
103 extracellular alkynes present in lipid II and newly-polymerized cell wall, we selected
104 picolyl azide-Cy3 as our label because the localized charge on the sulfonated cyanine
105 dye confers poor membrane permeability (*15*). Using this optimized protocol, we
106 observed nascent peptidoglycan deposition at the polar tip, whereas MurG-Dendra2
107 was more posterior (Fig. 2D). Our data support a model in which lipid II synthesis is
108 laterally and biochemically partitioned from the ensuing steps of peptidoglycan
109 assembly.

110 In the Gram-positive bacterium *Bacillus subtilis*, MurG associates with **r**egions of
111 **i**ncreased **f**luidity (RIFs) in the plasma membrane that are marked by the accumulation
112 of certain lipophilic fluorescent dyes (*16*). Benzyl alcohol has been used to disperse
113 plasma membrane domains in plant, animal and bacterial cells, including *B. subtilis*
114 RIFs (*16-18*). Mycobacteria are also Gram-positive but have a second 'myco'
115 membrane that is covalently attached to the cell wall. We found that benzyl alcohol did

116 not alter labeling by NalkTMM or OalkTMM (Fig. S9), which respectively incorporate into
117 the noncovalent and covalent mycolates of the mycomembrane (*19*). It did, however,
118 alter the distribution of FM4-64 (Fig. S6), a dye used previously to label the
119 mycobacterial plasma membrane (*20*), and altered glycolipid abundance in the IMD
120 (Fig. S7). MurG-Dendra2 was also notably less enriched in the IMD following benzyl
121 alcohol treatment (Fig. 1C) and, in live cells, at the cell poles (Fig. 3A). By contrast
122 benzyl alcohol produced subtle changes in the distribution of active PBPs, although
123 PonA1 shifted toward the poles in live cells (Fig. 3A). Disruption of plasma membrane
124 organization by benzyl alcohol was accompanied by delocalization of cell wall assembly
125 within 5 min (Fig. S8) as well as an overall reduction in synthesis (Fig. 3B, Figs. S8) and
126 halt in cell elongation (Fig. S9). The phenotypes were reversible: we recovered viable,
127 peptidoglycan-synthesizing cells following benzyl alcohol washout (Figs. S9, S10).
128 These data suggest that membrane partitioning is an essential feature of both
129 peptidoglycan synthesis and cell growth in *M. smegmatis*.
130 We find that benzyl alcohol also inhibits cell wall assembly in *B. subtilis* (Fig. 3C),
131 demonstrating that plasma membrane architecture may optimize peptidoglycan
132 biogenesis in bacterial phyla with divergent cell envelope structures and modes of
133 growth. Moreover, our previous work suggests that the biosynthetic pathways for
134 phosphatidylethanolamine, a major phospholipid of mycobacterial plasma membrane,
135 phosphatidylinositol mannoside, a cell envelope glycolipid, and menaquinone, the
136 primary lipid electron carrier of the mycobacterial respiratory chain, are partitioned
137 across the IMD and PM-CW (*5, 6, 21*). In the absence of a standard set of membrane-

138 bound organelles, plasma membrane compartmentalization may be a general bacterial
139 strategy for organizing pathways with lipid-linked intermediates and enzymes.
140

141 **Acknowledgments:** We are grateful to Drs. James Chambers and Amy Burnside for
142 microscopy and flow cytometry guidance and Ms. Sylvia Rivera for technical assistance.
143 We also thank Drs. Eric Strieter and Jiaan Liu for help in biotin-D-lysine (BDL)
144 preparation and Drs. Hesper Rego and Eric Rubin for *ponA1-mRFP*. We thank Dr.
145 Christopher Sassetti for the MurJ and MurG depletion strains, and Dr. Shana Topp for
146 providing the B. subtilis strain. We are grateful with Dr. Benjamin Swarts for providing
147 the OalkTMM and NalkTMM probes. Research was supported by funds from the
148 National Institutes of Health (NIH) under awards U01CA221230 and NIH DP2 AI138238
149 (M.S.S.) and R03 AI140259-01 (Y.S.M.), and R01 AI097191 (J.J. and T.A.G.). A.G.-H.
150 was supported by an Honors Fellowship from Universidad Autónoma de Nuevo León.
151 J.P. is a recipient of the Science Without Boarders Fellowship from CAPES-Brazil
152 (0328-13-8). Authors declare no competing interests. All data are available in the main
153 text or the supplementary materials.
154

155 **List of Supplementary Materials:**
156 Materials and Methods
157 Figures S1-S10
158 Tables S1
159

160 **Figure 1. MurG is enriched in the IMD.** (A) Membrane-bound steps of peptidoglycan
161 synthesis with hypothesized partitioning into the IMD and PM-CW. NAM, N-
162 acetylmuramic acid; NAG, N-acetylglucosamine; circles, amino acids: light green, L-ala;
163 red, D-glu; deep blue, diaminopimelic acid; yellow, D-ala. (B) Plasma membrane
164 fractionation. Bacteria are lysed by nitrogen cavitation and cell lysate is sedimented on
165 a sucrose density gradient. (C) Lysates from MurG-Dendra2-expressing *M. smegmatis*
166 were fractionated as in (B) and separated by SDS-PAGE. Protein detected by in-gel
167 fluorescence. Incubation of bacteria with 100 mM benzyl alcohol (BA) for 1 hour
168 decreased the enrichment of MurG-Dendra2 in the IMD. (D) *M. smegmatis*
169 coexpressing MurG-Dendra2 and mCherry-GlfT2 was imaged by structured illumination
170 microscopy (SIM-E, left). Fluorescence distribution of the fusion proteins from 59 cells
171 was quantitated from parallel conventional fluorescence microscopy (right). Signal was
172 normalized to the length and total fluorescence intensity of the cell. Cells were oriented
173 such that the brighter pole is on the right hand side of the graph. a.u., arbitrary units,
174 scalebar 5 μm.
175
176 **Figure 2. Lipid II is synthesized in the IMD and trafficked to the PM-CW**. (A)
177 Detection of lipid-linked peptidoglycan precursors from organic extracts of *M.*
178 *smegmatis* membrane fractions. Terminal D-alanines (yellow) of endogenous precursors
179 are exchanged for biotin-D-lysine (BDL; pink) via purified *S. aureus* PBP4. Biotinylated
180 species are detected by blotting with streptavidin-HRP. (B) Detection of peptidoglycan
181 precursors and PonA1 activity from density gradient fractions. Precursors are in both
182 the IMD and PM-CW in wildtype *M. smegmatis* but accumulate in the IMD upon MurJ

183 depletion (*10*). PonA1 binds Bocillin-FL in the PM-CW before or after 1 hour of 100 mM
184 benzyl alcohol treatment. (C) Wildtype *M. smegmatis* membrane fractions (50 µg/mL of
185 total protein each) were incubated with 40 µM Bocillin-FL and separated by SDS-PAGE.
186 Active PBPs detected by in-gel fluorescence in PM-CW. PonA1 was identified in Fig.
187 S3. (D) SIM-E of *M. smegmatis* coexpressing PonA1-mRFP and PimE-GFP, scalebar 5.
188 (E) Top, metabolic labeling of mycobacterial cell wall synthesis (*10*). Bottom, *M.*
189 *smegmatis* expressing MurG-Dendra2 were incubated with alkDADA for 2 min (~1%
190 generation). Surface-exposed alkynes on fixed cells were detected by CuAAC with
191 picolyl azide-Cy3 (*10*). Cells imaged by SIM-E, scalebar 5 µm.
192
193 **Figure 3. Perturbation of plasma membrane organization disrupts peptidoglycan**
194 **biogenesis**. (A) *M. smegmatis* coexpressing PonA1-mRFP and MurG-Dendra2 were
195 imaged +/- benzyl alcohol by SIM-E (left). Fluorescence distribution of the fusion
196 proteins from 42<n<56 cells was quantitated from parallel conventional fluorescence
197 microscopy (right). Signal was normalized as Fig. 1D, scalebar 5 µm. (B) Wildtype *M.*
198 *smegmatis* +/- benzyl alcohol were incubated with both azido D-amino acid dipeptide
199 and mycomembrane probe OalkTMM (*10, 19*) for 15 min and fixed in 2% formaldehyde.
200 Alkynes and azides were detected by sequential CuAAC reactions with picolyl azide
201 TAMRA and alkyne carboxyrhodamine 110 (Click Chemistry Tools) labels with a wash
202 step between, scalebar 5 µm. (C) *B. subtilis* were exposed to indicated antibiotics or
203 benzyl alcohol for 10 min then incubated with alkDADA for an additional 5 min. Cells
204 were fixed and alkynes were detected by CuAAC with picolyl azide CR 110. MFI,
205 median fluorescence intensity obtained by flow cytometry. Experiments performed three

206 times in triplicate. Error bars, +/- standard deviation of biological replicates. ***, $p < 0.0005$; ****, $p < 0.00005$, Tukey multiple comparison test.

208

209 **References:**

210 1. C. L. Gee *et al.*, A phosphorylated pseudokinase complex controls cell wall
211 synthesis in mycobacteria. *Sci Signal* **5**, ra7 (2012).
212 2. A. J. Meeske *et al.*, SEDS proteins are a widespread family of bacterial cell wall
213 polymerases. *Nature* **537**, 634-638 (2016).
214 3. K. Emami *et al.*, Corrigendum: RodA as the missing glycosyltransferase in
215 *Bacillus subtilis* and antibiotic discovery for the peptidoglycan polymerase
216 pathway. *Nature Microbiology* **2**, 17019 (2017).
217 4. D. Arora *et al*., The transpeptidase PbpA and non-canonical transglycosylase
218 RodA of Mycobacterium tuberculosis play important roles in regulating bacterial
219 cell lengths. *J Biol Chem*, jbc. M117. 811190 (2018).
220 5. Y. S. Morita *et al.*, Compartmentalization of lipid biosynthesis in mycobacteria. *J*
221 *Biol Chem* **280**, 21645-21652 (2005).
222 6. J. M. Hayashi *et al.*, Spatially distinct and metabolically active membrane domain
223 in mycobacteria. *Proc Natl Acad Sci U S A* **113**, 5400-5405 (2016).
224 7. J. M. Hayashi *et al.*, Stress-Induced Reorganization of the Mycobacterial
225 Membrane Domain. *mBio* **9**, (2018).
226 8. X. Meniche *et al.*, Subpolar addition of new cell wall is directed by DivIVA in
227 mycobacteria. *Proc Natl Acad Sci U S A* **111**, E3243-3251 (2014).

228 9. Y. Qiao *et al.*, Detection of lipid-linked peptidoglycan precursors by exploiting an
229 unexpected transpeptidase reaction. *J Am Chem Soc* **136**, 14678-14681 (2014).
230 10. A. García-Heredia *et al.*, Peptidoglycan precursor synthesis along the sidewall of
231 pole-growing mycobacteria. *eLife* **7**, (2018).
232 11. Y. Qiao *et al.*, Lipid II overproduction allows direct assay of transpeptidase
233 inhibition by beta-lactams. *Nat Chem Biol* **13**, 793-798 (2017).
234 12. E. C. Hett *et al*., Interaction and modulation of two antagonistic cell wall enzymes
235 of mycobacteria. *PLoS Pathog* **6**, e1001020 (2010).
236 13. K. J. Kieser *et al.*, Phosphorylation of the peptidoglycan synthase PonA1 governs
237 the rate of polar elongation in mycobacteria. *PLoS Pathog* **11**, e1005010 (2015).
238 14. G. W. Liechti *et al.*, A new metabolic cell-wall labelling method reveals
239 peptidoglycan in *Chlamydia trachomatis*. *Nature* **506**, 507-510 (2014).
240 15. N. J. Yang, M. J. Hinner, Getting across the cell membrane: an overview for
241 small molecules, peptides, and proteins. *Methods in Molecular Biology (Clifton,*
242 *N.J.)* **1266**, 29-53 (2015).
243 16. A. Muller *et al.*, Daptomycin inhibits cell envelope synthesis by interfering with
244 fluid membrane microdomains. *Proc Natl Acad Sci U S A* **113**, E7077-e7086
245 (2016).
246 17. B. L. Orvar *et al*., Early steps in cold sensing by plant cells: the role of actin
247 cytoskeleton and membrane fluidity. *The Plant Journal* **23**, 785-794 (2000).
248 18. E. Nagy *et al.*, Hyperfluidization-coupled membrane microdomain reorganization
249 is linked to activation of the heat shock response in a murine melanoma cell line.
250 *Proc Natl Acad Sci U S A* **104**, 7945-7950 (2007).

251 19. H. N. Foley *et al*., Bioorthogonal chemical reporters for selective in situ probing of
252 mycomembrane components in mycobacteria. *Angewandte Chemie* **128**, 2093-
253 2097 (2016).
254 20. X. Zhou *et al.*, Sequential assembly of the septal cell envelope prior to V
255 snapping in *Corynebacterium glutamicum*. *Nature Chemical Biology*, 1 (2019).
256 21. J. Puffal *et al.*, Demethylmenaquinone Methyl Transferase Is a Membrane
257 Domain-Associated Protein Essential for Menaquinone Homeostasis in
258 *Mycobacterium smegmatis*. *Frontiers in Microbiology* **9**, 3145 (2018).
259 22. Y. S. Morita *et al.*, PimE is a polyprenol-phosphate-mannose-dependent
260 mannosyltransferase that transfers the fifth mannose of phosphatidylinositol
261 mannoside in mycobacteria. *Journal of Biological Chemistry*, (2006).
262 23. C. B. Sena *et al.*, Controlled expression of branch-forming mannosyltransferase
263 is critical for mycobacterial lipoarabinomannan biosynthesis. *Journal of Biological*
264 *Chemistry*, M109. 077297 (2010).
265 24. J. Schindelin *et al.*, Fiji: an open-source platform for biological-image analysis.
266 *Nature Methods* **9**, 676-682 (2012).
267 25. A. Paintdakhi *et al.*, Oufti: an integrated software package for high-accuracy,
268 high-throughput quantitative microscopy analysis. *Mol Microbiol* **99**, 767-777
269 (2016).
270

Figure 1

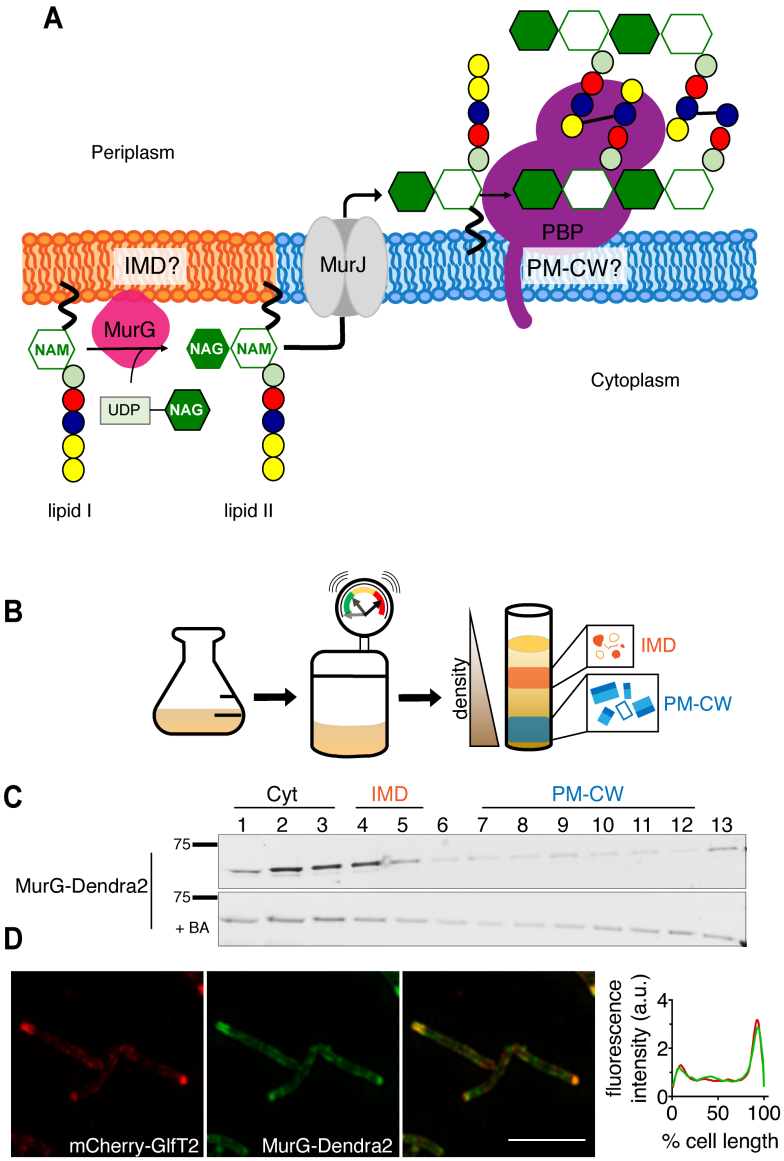
A
Periplasm
IMD?
MurG
NAM
NAG
NAM
UDP
NAG
MurJ
PBP
PM-CW?
Cytoplasm
lipid I
lipid II
B
density
IMD
PM-CW
C
Cyt
IMD
PM-CW
1 2 3 4 5 6 7 8 9 10 11 12 13
75
MurG-Dendra2
75
+ BA
D
mCherry-GlfT2
MurG-Dendra2
fluorescence intensity (a.u.)
4
2
0
0 50 100
% cell length

Figure 2

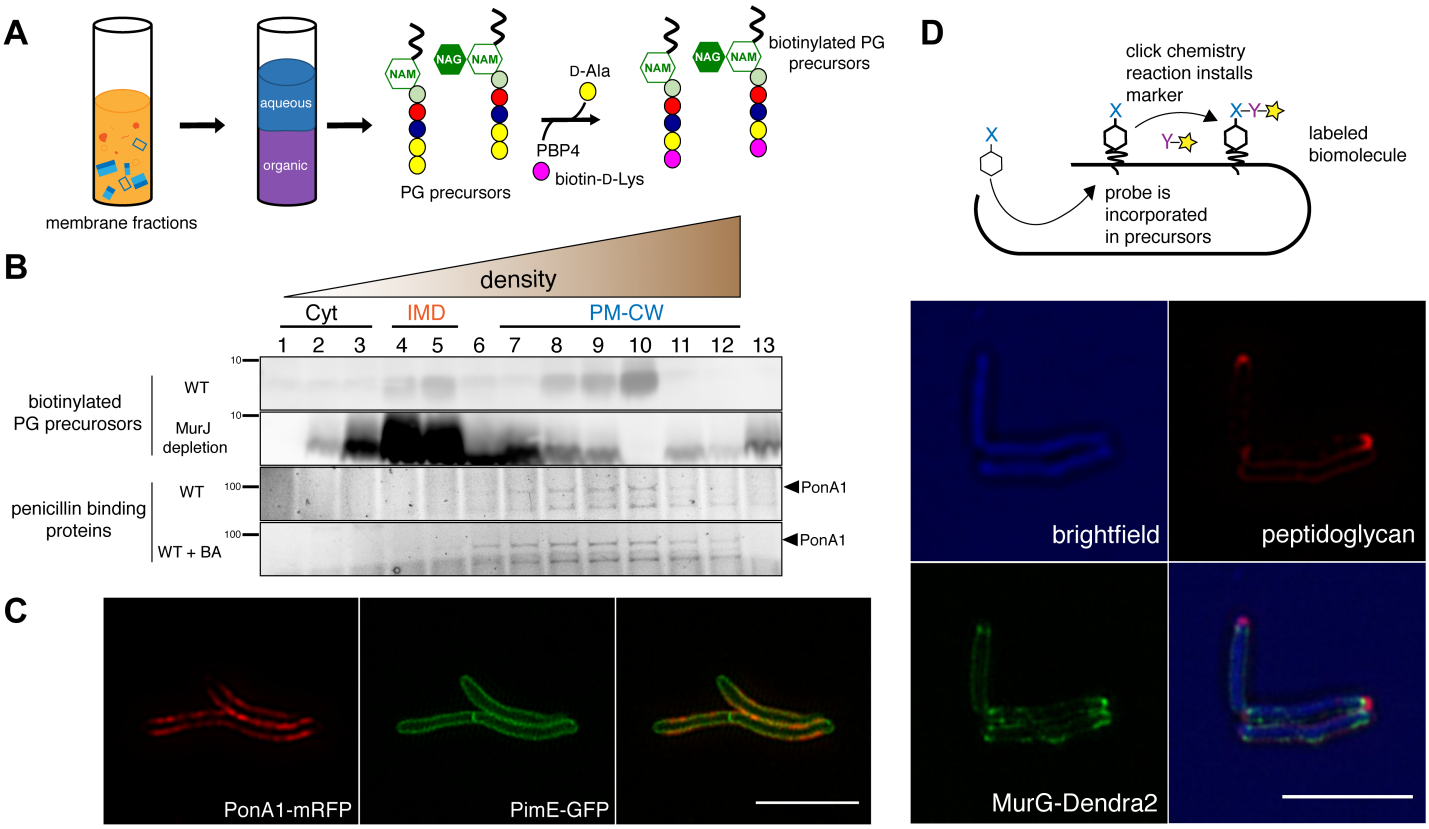
A
membrane fractions
aqueous
organic
NAM
NAG
PG precursors
D-Ala
PBP4
biotin-D-Lys
biotinylated PG precursors
B
density
Cyt
IMD
PM-CW
1 2 3 4 5 6 7 8 9 10 11 12 13
biotinylated PG precurosors
WT
MurJ depletion
penicillin binding proteins
WT
WT + BA
PonA1
C
PonA1-mRFP
PimE-GFP
D
click chemistry reaction installs marker
X
X–Y
Y
labeled biomolecule
probe is incorporated in precursors
brightfield
peptidoglycan
MurG-Dendra2

Figure 3

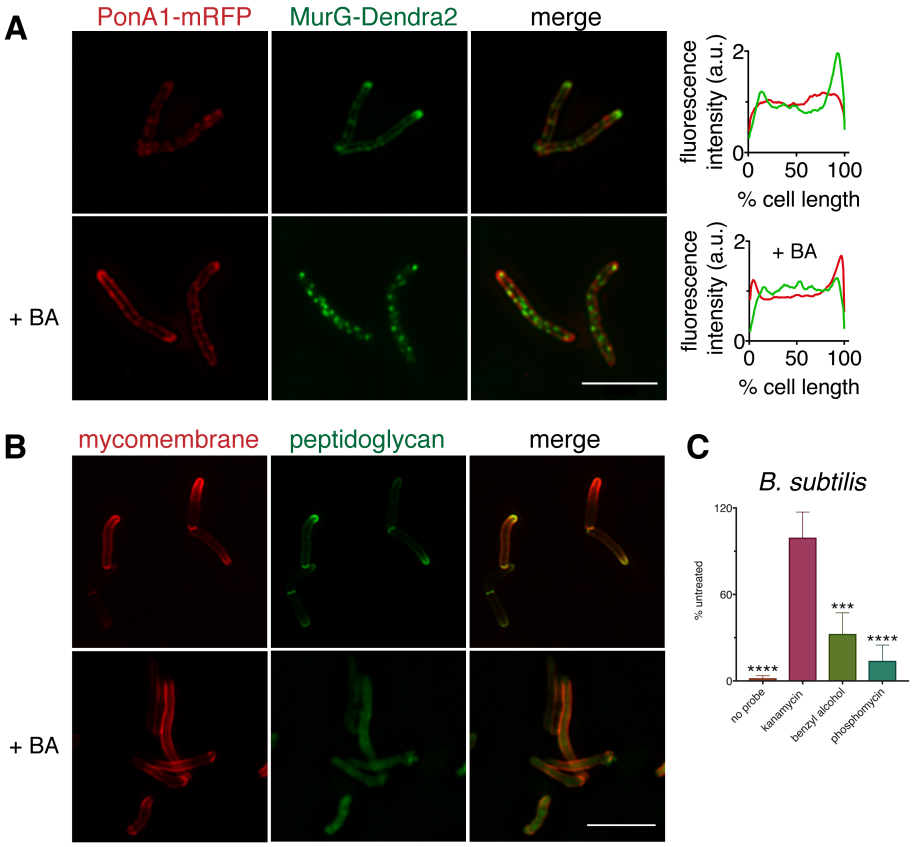
A
PonA1-mRFP
MurG-Dendra2
merge
+ BA
fluorescence intensity (a.u.)
% cell length
B
mycomembrane
peptidoglycan
merge
+ BA
C
B. subtilis
% untreated
no probe
kanamycin
benzyl alcohol
phosphomycin